

Study of Central Intensity Ratio of Seyfert Galaxies in nearby Universe

K T Vinod¹, C Baheej¹, S Aswathy² and C D Ravikumar¹

¹ Department of Physics, University of Calicut, Malappuram-673635, India; *vinod2085@gmail.com*

² Department of Physics, Providence Women's College, Calicut-673009, India

Received 20xx month day; accepted 20xx month day

Abstract We use the recently discovered simple photometric parameter Central Intensity Ratio (CIR, Aswathy & Ravikumar 2018) determined for a sample of 57 nearby ($z < 0.02$) Seyfert galaxies to explore the central features of galaxies and their possible connection with galaxy evolution. The sample of galaxies shows strong anti-correlation between CIR and mass of their central supermassive black holes (SMBH). The SMBH masses of ellipticals are systematically higher for a given CIR value than that for lenticulars and spirals in the sample. However, the correlation between CIR and central velocity dispersion is weak. CIR appears less influenced by the excess flux produced by the central engine in these galaxies, when compared to spectroscopic parameters like velocity dispersion and OIV flux, and proves a fast and reliable tool for estimating central SMBH mass.

Key words: Seyfert galaxies: photometry – galaxies: evolution – AGN: super massive black-hole

1 INTRODUCTION

The central supermassive black hole (SMBH) residing in massive galaxies is believed to play a key role in the evolution scenario of host galaxies. The evolution mechanism of the central engine of every galaxy is connected with the star formation process in the host galaxy. It is commonly accepted that the accretion mechanism is the prime reason for the origin and growth of active galactic nuclei (AGN) in the nuclear region of galaxies (Kawakatu et al. 2006; Ellison et al. 2011; Silverman et al. 2011; Villforth et al. 2012).

AGNs are hosted at the centre of elliptical galaxies or bulge dominating spheroids across all redshifts (Kauffmann et al. 2003; Pović et al. 2009), whereas the morphology of local Seyfert galaxies is generally spiral (Ho et al. 1995; Ho 2008). Intense circumnuclear star formation plays a crucial role in the evolution and emission process of Seyfert galaxies, specifically, Sy2 galaxies. (e.g., Terlevich & Melnick 1985; Maiolino et al. 1998; Cid Fernandes & Terlevich 1995; González Delgado et al. 2001; Cid Fernandes et al. 2001).

Seyfert galaxies are among the most studied objects in the radio-quiet (RQ) category, along with quasars (Weedman 1977; Osterbrock & Martel 1993; Rashed et al. 2015). The role of feedback by the central SMBH in the relationships between the mass of the SMBH and bulge properties of Seyfert galaxies is still unclear because the merger events govern the formation of bulges while Seyfert galaxies are believed to be evolving through secular evolution (Hopkins et al. 2006; Kormendy & Ho 2013; Heckman & Best 2014). Recent studies revealed the existence of fast outflows of ionized gas in nearby Seyfert galaxies, but their influence on star formation is still under debate (Christensen et al. 2006; Krause et al. 2007; Wang et al. 2012; García-Burillo et al. 2014; Morganti et al. 2015; Querejeta et al. 2016). However, if the host galaxies possess such outflows, they could expel the gas from the central region and suppress the star formation (Alexander & Hickox 2012; García-Burillo et al. 2014; Alatalo et al. 2015; Hopkins et al. 2016; Wylezalek & Zakamska 2016).

The masses of central supermassive black holes (SMBHs) are reported to correlate well with the stellar mass and stellar velocity dispersion of the bulges of their host galaxies (see, e.g., Magorrian et al. 1998; Ferrarese & Merritt 2000; Gebhardt et al. 2000; Marconi & Hunt 2003; Häring & Rix 2004; Kormendy & Ho 2013; McConnell & Ma 2013; Savorgnan & Graham 2015). The bulges and supermassive black holes seem to evolve together and regulate each other (Alonso-Herrero et al. 2013). The relations (between M_{BH} , bulge mass, and stellar velocity dispersion) propose a strong connection between the formation of black hole mass, emergence of AGNs, and the host galaxy evolution (Ferrarese & Merritt 2000; Gültekin et al. 2009) as well.

Central light concentration is a vital parameter, which can be used as a tracer of the disk to bulge ratio, star formation activity, and galaxy evolution (Abraham et al. 1994; Conselice 2003). The Central Intensity Ratio (CIR), a new photometric parameter, is well correlated with the masses of central SMBHs of the spheroid of early-type galaxies (Aswathy & Ravikumar 2018). Furthermore, CIR is an efficient photometric tool to study the central and structural properties of spiral galaxies, especially barred systems, and also gives some valid information regarding nuclear star formation and AGN formalism in host galaxies (Aswathy & Ravikumar 2020). In this light, we perform an optical analysis by utilizing the parameter, CIR, to study the central properties and evolution of Seyfert galaxies.

This paper is organized as follows; Section 2 describes the properties of the sample galaxies and the data reduction techniques employed in this study, and Section 3 deals with results consisting of various correlations. Discussions and conclusions are provided in Section 4.

Throughout this paper, we have used the cosmological parameters: $H_0 = 73.0 \text{ km s}^{-1} \text{ Mpc}^{-1}$; $\Omega_{\text{matter}} = 0.27$; $\Omega_{\text{vacuum}} = 0.73$.

2 THE DATA AND DATA REDUCTION

For this work, we consider a complete sample of Seyfert galaxies drawn from the Revised Shapley-Ames catalog (RSA Shapley & Ames 1932; Sandage & Tamman 1987) analyzed by Diamond-Stanic et al. (2009); Diamond-Stanic & Rieke (2012), which include 114 nearby ($z < 0.02$) Seyfert galaxies brighter than $B_T = 13.2$. We took archival images of the sample observed by the Hubble Space Telescope (HST) to estimate CIR. Among the 114 galaxies, 83 had HST observations in optical bands. From this, 13 galaxies

Table 1: Table 1 lists the properties of sample galaxies. Name of the galaxy (column 1), Distance (2), Seyfert type (3), Morphology (4), CIR computed in the corresponding filter (5), uncertainty of CIR (6), SMBH mass (7) and corresponding references (8), stellar velocity dispersion adopted from Hyperleda (9), OIV flux taken from Diamond-Stanic et al. (2009) (10), estimated circumnuclear SFR (11), uncertainty of SFR (12), HST observation (13).

Galaxy	Distance (Mpc)	Seyfert type	Morphology	CIR	Δ CIR	$\log M_{\text{BH}}$ (M_{\odot})	ref	σ (km s $^{-1}$)	OIV flux (erg cm $^{-2}$ s $^{-1}$)	$\log \text{SFR}$ (M_{\odot} yr $^{-1}$)	Δ SFR	HST obs.
IC2560	40.7	S2	(R')SB(r)b	1.44	0.03	6.64	1	136.5	5.43E-013	0.67	0.013	WFPC2_F814
IC3639	35.3	S2	SB(rs)bc	1.27	0.02	6.83	2	97.1	3.55E-013	1.64	0.040	WFPC2_F606
NGC0613	20.7	S?	SB(rs)bc	0.86	0.02	7.60	3	122.1	—	0.91	0.007	WFPC2_F814
NGC0788	54.1	S2	SA(s)0/a	1.16	0.03	7.51	2	134.4	1.80E-013	1.01	0.021	WFPC2_F606
NGC1275	70.1	S2	E-cD	1.07	0.03	8.58	2	244.6	1.85E-013	2.22	0.170	WFPC2_F702
NGC1358	53.6	S2	SAB(r)0/a	1.17	0.02	7.88	2	215.1	7.61E-014	—	—	WFPC2_F606
NGC1365	21.5	S1.8	SB(s)b	1.78	0.03	6.05	4	141.1	1.58E-012	1.06	0.009	WFPC2_F814
NGC1386	10.6	S2	SB0+(s)	1.10	0.02	7.23	2	133.1	8.70E-013	-0.11	0.001	WFPC2_F814
NGC1399	19.4	S2	E1 pec	0.58	0.01	8.94	3	332.2	—	—	—	WFPC2_F814
NGC1433	13.3	S2	(R')SB(r)ab	0.91	0.02	7.24	5	107	6.07E-014	0.38	0.002	WFPC2_F814
NGC1566	19.4	S1.5	SAB(s)bc	1.03	0.03	7.11	4	97.7	8.88E-014	0.67	0.005	WFPC2_F814
NGC1667	61.2	S2	SAB(r)c	1.09	0.03	7.88	2	169.4	9.28E-014	1.51	0.049	WFPC2_F606
NGC1672	16.7	S2	SB(s)b	0.77	0.02	7.70	6	109.5	—	1.35	0.010	WFPC2_F814
NGC1808	12.3	S2	(R)SAB(s)a	0.90	0.02	7.20	7	126.1	—	-0.11	0.001	WFPC2_F814
NGC2273	28.4	S2	SB(r)a	1.15	0.03	7.30	2	141	1.47E-013	0.14	0.004	WFPC2_F791
NGC2639	42.6	S1.9	(R)SA(r)a	0.69	0.03	7.94	2	175.3	3.27E-014	0.43	0.009	WFPC2_F814
NGC2782	37	S2	SAB(rs)a pec	1.21	0.03	7.70	8	182.2	—	1.81	0.032	WFPC2_F814
NGC2974	20.9	S2	E4	1.20	0.02	8.23	9	232.2	—	—	—	WFPC2_F814
NGC3081	34.2	S2	(R)SAB(r)0/a	0.88	0.03	7.20	3	118.8	9.89E-013	—	—	WFPC2_F814
NGC3169	17.4	S	SA(s)a pec	0.74	0.02	8.01	10	184.9	—	-0.42	0.001	WFPC2_F814
NGC3185	21.3	S2	(R)SB(r)a	1.58	0.03	6.52	2	76.1	4.70E-014	-0.44	0.001	WFPC2_F814
NGC3227	20.6	S1.5	SAB(s)a pec	1.66	0.00	6.75	11	126.8	5.71E-013	—	—	ACS_F814
NGC3281	44.7	S2	SA(s)ab pec	0.86	0.04	7.28	2	168.6	1.39E-012	—	—	WFPC2_F606
NGC3486	7.4	S2	SAB(r)c	1.10	0.03	7.00	12	60.2	3.30E-014	-0.41	0.001	WFPC2_F814
NGC3489	6.73	S2	SAB0+(rs)	1.34	0.01	6.78	13	104.2	—	-0.41	0.001	WFPC2_F814
NGC3516	38.9	S1.2	(R)SB(s)0	1.45	0.02	7.23	24	153.6	5.60E-013	1.83	0.037	WFPC2_F791
NGC3982	17	S1.9	SAB(r)b	1.12	0.03	7.20	14	71.8	1.18E-013	—	—	WFPC2_F814
NGC4168	16.8	S1.9	E2	0.74	0.04	9.01	15	182	1.39E-014	—	—	WFPC2_F702
NGC4235	35.1	S1.2	SA(s)a	0.99	0.03	7.64	2	133.6	4.33E-014	-0.17	0.003	WFPC2_F606
NGC4258	8	S1.9	SAB(s)bc	0.72	0.08	7.58	2	132.8	7.49E-014	0.25	0.001	ACS_F814
NGC4303	13.6	S2	SAB(rs)bc	1.69	0.01	6.58	16	95.1	—	—	—	WFPC2_F814
NGC4374	18.5	S2	E1	0.60	0.01	8.97	1	277.6	—	—	—	WFPC2_F814
NGC4472	17.1	S2	E2	0.53	0.02	9.18	17	282	6.64E-014	—	—	WFPC2_F814
NGC4477	16.8	S2	SB0(s)	0.79	0.02	7.91	2	172.5	1.69E-014	0.08	0.002	WFPC2_F606
NGC4501	16.8	S2	SA(rs)b	1.22	0.02	7.30	3	166.2	3.98E-014	0.02	0.004	WFPC2_F606
NGC4507	59.6	S2	(R')SAB(rs)b	1.34	0.02	7.58	2	149	3.31E-013	—	—	WFPC2_F814
NGC4552	15.4	S2	E0-1	0.91	0.01	8.63	18	250.3	—	—	—	WFPC2_F814
NGC4579	16.8	S1.9	SAB(rs)b	1.13	0.02	7.70	19	165.8	2.83E-014	0.22	0.004	WFPC2_F791
NGC4594	20	S1.9	SA(s)a	0.91	0.01	8.76	2	225.7	2.62E-014	0.38	0.003	WFPC2_F814
NGC4698	16.8	S2	SA(s)ab	1.03	0.02	7.61	2	137.4	2.03E-014	-0.53	0.001	WFPC2_F814
NGC4725	12.4	S2	SAB(r)ab pec	0.87	0.01	7.51	2	131.5	1.24E-014	-0.01	0.002	WFPC2_F606
NGC5005	21.3	S2	SAB(rs)bc	0.60	0.00	7.84	20	171.5	1.99E-014	1.91	0.013	ACS_F814

Galaxy	Distance (Mpc)	Seyfert type	Morphology	CIR	Δ CIR	$\log M_{\text{BH}}$ (M_{\odot})	ref	σ (km s $^{-1}$)	OIV flux (erg cm $^{-2}$ s $^{-1}$)	$\log \text{SFR}$ ($M_{\odot} \text{ yr}^{-1}$)	ΔSFR	HST obs.
NGC5033	18.7	S1.9	SA(s)c	0.96	0.02	7.64	2	133.9	1.59E-013	-0.28	0.001	WFPC2_F814
NGC5135	57.7	S2	SB(s)ab	1.11	0.02	7.34	2	125.5	5.83E-013	1.95	0.069	WFPC2_F606
NGC5194	8.4	S2	SA(s)bc pec	1.27	0.02	6.95	2	87.9	2.46E-013	-0.62	0.000	WFPC2_F814
NGC5273	21.3	S1.5	SA0(s)	1.47	0.03	6.61	3	65.9	3.72E-014	-0.10	0.001	WFPC2_F791
NGC5322	24.3	S	E3-4	0.96	0.02	8.51	21	230	—	—	—	WFPC2_F814
NGC5427	40.4	S2	SA(s)c pec	1.16	0.03	7.58	3	69.9	2.68E-014	1.00	0.013	WFPC2_F606
NGC5643	14.4	S2	SAB(rs)c	1.45	0.02	6.44	22	—	8.16E-013	—	—	WFPC2_F814
NGC5806	27.4	S2	SAB(s)b	1.10	0.03	7.07	23	124.3	—	—	—	WFPC2_F814
NGC6814	25.6	S1.5	SAB(rs)bc	1.29	0.03	7.26	2	108.1	2.13E-013	1.55	0.025	WFPC2_F606
NGC6951	24.1	S2	SAB(rs)bc	0.73	0.02	7.34	2	114.8	8.37E-014	0.60	0.014	WFPC2_F814
NGC7469	67	S1.2	(R')SAB(rs)a	1.06	0.00	7.08	2	132.9	3.67E-013	2.99	0.281	ACS_F814
NGC7479	32.4	S1.9	SB(s)c	0.85	0.04	7.68	2	151.3	2.67E-013	—	—	WFPC2_F814
NGC7582	22	S2	(R')SB(s)ab	1.84	0.02	7.74	2	118.4	2.22E-012	-0.10	0.002	WFPC2_F606
NGC7590	22	S2	SA(rs)bc	1.09	0.02	6.79	2	91.5	6.88E-014	0.52	0.005	WFPC2_F606
NGC7743	24.4	S2	(R)SB0+(s)	1.49	0.02	6.72	2	83.5	3.30E-014	—	—	WFPC2_F606

References:(1)Kormendy & Ho (2013) (2)Diamond-Stanic & Rieke (2012) (3)van den Bosch (2016) (4)Davis et al. (2014) (5)Smajic et al. (2014) (6)Combes et al. (2019) (7)Busch et al. (2017) (8)Dong & De Robertis (2006) (9)Savorgnan & Graham (2016) (10)Dong & Wu (2015) (11)Onken et al. (2003) (12)Koliopanos et al. (2017) (13)Nowak et al. (2010) (14)Beifiori et al. (2012) (15)Magorrian et al. (1998) (16)Davis et al. (2018) (17)Graham & Soria (2019) (18)Pellegrini (2010) (19)Barth et al. (2001) (20)Izumi et al. (2016) (21)Dullo et al. (2018) (22)Goulding et al. (2010) (23)Dumas et al. (2007).

consisting of bad pixels or defects on their images within the region of central 3 arcsecs are avoided from the sample. Also, we excluded 10 small galaxies, in which the size of their images is less than the 3 arcsecs aperture, and 3 highly inclined galaxies ($i > 70^{\circ}$). The final sample consists of 57 Seyfert galaxies comprising 40 spiral, 9 lenticular, and 8 elliptical galaxies. We chose galaxy images observed with Wide Field Planetary Camera 2 (WFPC2). It is already reported that though there exist slight variations among values of CIR estimated from nearby filters, the variations are not strong enough to disrupt the observed correlations involving CIR (Sruthi & Ravikumar 2021). Hence we included observations using all filters of WFPC2 from F606W to F814W, giving preference to the filter in the highest wavelength region available. Further, we added four observations using F814W with Advanced Camera for Surveys to improve the statistics for which no WFPC2 images were available. Since the sample galaxies possess AGN, we have checked the central region of the sample galaxies by constructing residual images using the *ellipse* task in IRAF. Many sub structures like bar, ring, spiral-arms are visible in the residual image, however, no significant optical excess flux could be identified in these galaxies that could affect determination of CIR.

Following Aswathy & Ravikumar (2018), the CIR is determined for the sample galaxies by using the aperture photometry (MAG_APER) technique, which is provided in source extractor (SExtractor, Bertin & Arnouts 1996).

$$\text{CIR} = \frac{I_1}{I_2 - I_1} = \frac{10^{0.4(m_2 - m_1)}}{1 - 10^{0.4(m_2 - m_1)}} \quad (1)$$

where I_1 and I_2 are the intensities and m_1 and m_2 are the corresponding magnitudes of the light within the inner and outer apertures of radii R_1 and R_2 , respectively. The inner radius is chosen such that its a few

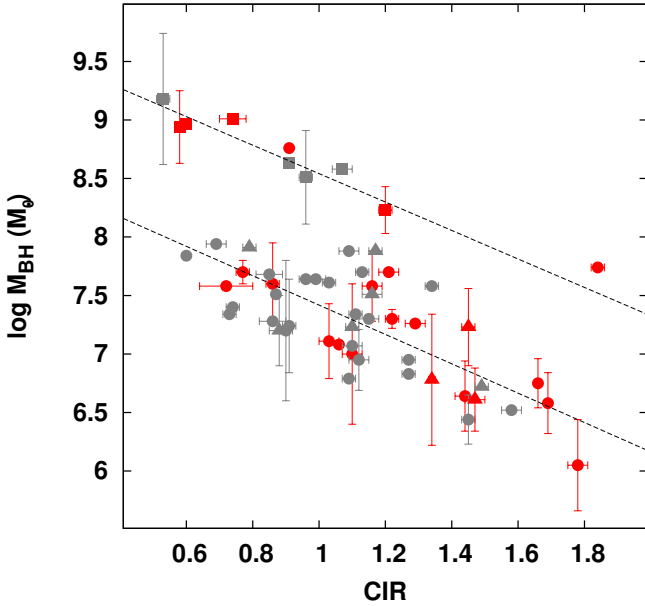


Fig. 1: Correlation between the central intensity ratio and mass of the SMBH of the sample galaxies. Filled circles, triangles, and squares represent spiral, lenticular, and elliptical galaxies, respectively. Estimations of masses of SMBH using dynamical methods are denoted as red data points, while gray color is used to represent those from the stellar velocity dispersion measurements of host galaxies.

times the PSF. The outer radius (conventionally $2R_1$) is chosen such that the aperture is lying fairly within the galaxy image. For the sample, we chose the inner and outer radii as 1.5 and 3 arcsecs, respectively.

Ultraviolet (UV) observations are vital in providing recent star formation activity in galaxies (e.g., Gil de Paz et al. 2005, 2007; Thilker et al. 2005; Koribalski & López-Sánchez 2009). For the estimation of circumnuclear star formation rate (SFR), we took far-UV (FUV, 1350-1750 Å) data of the sample galaxies observed by the GALaxy Evolution eXplorer (GALEX) mission. We used an aperture size of 10 arcsecs at the centre of the image to estimate the circumnuclear SFR following López-Sánchez (2010) using the calibration provided by Salim et al. (2007) and is provided in Table 1.

3 RESULTS

Scaling relations displayed by various structural and dynamical observables of galaxies can shed vital information on formation and evolution processes in galaxies. We have estimated the CIR at the optical centre of 57 Seyfert galaxies observed using HST. The sample properties, along with the estimated values of CIR, are tabulated in Table 1. We next explore various trends involving CIR.

3.1 Variation of CIR with SMBH mass

The scaling relations of black hole mass are generally determined and explored utilizing the bulge properties of the host galaxies, specifically in early-type galaxies (Kormendy & Richstone 1995; Ferrarese & Merritt 2000; McConnell & Ma 2013). Structural properties of late-type galaxies, like the pitch angle of spiral arms, share intriguing scaling relation with the black hole mass (Davis et al. 2018, 2019).

Figure 1 shows the variation of CIR with mass of SMBH for the sample galaxies. Filled circles, triangles, and squares represent spiral, lenticular, and elliptical galaxies, respectively. We find a strong correlation between the CIR of the Seyfert galaxies and the mass of their central SMBH. However, the early-type galaxies in the sample host systematically high black hole mass when compared to lenticulars and spirals, for the same value of CIR considered. The Pearson's linear correlation coefficient, r , for the correlation exhibited by spirals and lenticulars together is -0.74 with a significance, s , > 99.99 per cent (Press et al. 1992) while that for elliptical galaxies is -0.94 with a significance of 99.40 per cent.

Two galaxies, NGC4594 and NGC7582, show significant deviation from this correlation. NGC4594, the Sombrero galaxy, is reported to have an unusually large bulge mass and a very massive SMBH at the centre of the galaxy. It is usually classified as a normal spiral, Sa, galaxy (de Vaucouleurs et al. 1991) but following many scaling relations of ellipticals (Gadotti & Sánchez-Janssen 2012). NGC7582 is reported to host a ring with active star formation within the pc scale radius (≈ 190 pc) surrounding the nucleus of the galaxy, along with a high stellar velocity dispersion (Riffel et al. 2009). The intense nuclear starburst activity (Cid-Fernandes et al. 2001; Bianchi et al. 2007) can affect its CIR value.

In Section 3.2, we notice that there is no apparent correlation between CIR and stellar velocity dispersion of host galaxies in our sample, even though the latter and mass of SMBH are reported to share a strong correlation. In order to explore this discrepancy, we also employed a color code to distinguish the method adopted to estimate the masses of SMBH. Masses estimated using a dynamical method (e.g., reverberation mapping, stellar dynamics, maser dynamics and gas dynamics) are shown in red while mass estimations based on stellar velocity dispersion are shown in gray in Figure 1. If we include only dynamically estimated masses, the correlation coefficient improves to -0.77 at a significance, s = 99.97 per cent, while it reduces drastically to -0.68 (s = 99.98 per cent) when these data points are excluded.

3.2 Variation between the CIR and σ

The variation of CIR with the stellar velocity dispersion of the sample galaxies is shown in Figure 2(a). As already mentioned, there is no significant correlation between CIR and stellar velocity dispersion (σ) of Seyfert galaxies. However, if we exclude the eight early-type galaxies in the sample, the velocity dispersion measurements of galaxies with dynamical estimation of SMBH (red triangles and circles) show larger scatter compared to their gray counterparts. Such a discrepancy is not clear in early-type galaxies. The extreme emission from AGN activity can complicate the measurement of central velocity dispersion in these galaxies (Riffel et al. 2013).

Measurements of stellar velocity dispersion may be biased by the contribution of rotating stellar disks because of the rotational broadening of the stellar absorption lines and the velocity dispersion measurements could be noticeably increased by the rotational effect (Woo et al. 2015). Due to higher velocity-to-dispersion (V/σ) ratios, the rotational effect is significantly more prominent in late-type galaxies (LTGs) than in ETGs.

3.3 Variation between the CIR and SFR

In Figure 2(b), we explore the connection between CIR and circumnuclear SFR traced by the UV luminosity (FUV) in an aperture of radius 10 arcsec at the galactic centre. We find that there is no correlation

Table 2: The table lists the best-fitting parameters for the relation $x = \alpha \text{ CIR} + \beta$ and correlation coefficients for various relations.

x	α	β	r	s	n
$\log M_{\text{BH}}$	-1.25±0.16	8.67±0.19	-0.74	> 99.99%	47
(spiral+lenticular)					
$\log M_{\text{BH}}$	-1.16±0.15	9.67±0.13	-0.94	99.40%	8
(elliptical)					
$\log \text{OIV flux}$	1.49±0.24	-14.60±0.28	0.70	> 99.99%	38

between CIR and circumnuclear SFR. The properties of sub-structures in the nuclear region of host galaxies may influence the star formation process, and there by affecting CIR. The galaxies IC2560, NGC0788, NGC1667, NGC3516, NGC5427, and NGC6814, denoted by the numbers 1 to 6 respectively in the figure, possess nuclear dust spirals, which can regulate the nuclear SFR at the central region of the galaxies (Muñoz Marín et al. 2007; Evans et al. 1996; Martini et al. 2003; Pérez-Ramírez et al. 2000). The galaxies IC3639, NGC2782, NGC5135, and NGC7582, numbered 7 to 10, with nuclear start burst activity (Boer et al. 1992; González Delgado et al. 2001; Muñoz Marín et al. 2007; Bianchi et al. 2007) are also apparent outliers in the figure. NGC1365 and NGC7469 are the galaxies showing intense nuclear SFR, with star-forming regions concentrated in hot spots around the nucleus (Ramos Almeida et al. 2009; Davies et al. 2007), which are shown in the figure by the numbers 11 and 12. By excluding these galaxies, we may see a negative trend in CIR and SFR. However, it is insufficient to confirm any connection between CIR and SFR, necessitating a thorough investigation with larger sample size.

3.4 Variation between the CIR and OIV flux

In Figure 2(c), we show the observed correlation between CIR and OIV flux of the host galaxy, which is taken from Diamond-Stanic et al. (2009). OIV flux is an accurate measure of intrinsic AGN luminosity (Diamond-Stanic et al. 2009) and we find a positive correlation with CIR ($r = 0.70$ with $s > 99.99$ per cent). OIV emission ($25.9 \mu\text{m}$) is a tracer of highly ionized gas of the order of 35-97 eV, and these types of mid-IR emission lines can be produced in the vicinity of hot stars in the central region of AGN host galaxies (Pottasch et al. 2001; Smith et al. 2004; Devost 2007). AGN luminosity depends upon the fuel consumed by the SMBH at the nuclear region of the galaxy, and early-type galaxies have less fuel than the late-type galaxies (Rieke 2002). This suggests that AGN power is likely to decrease while SMBH grows in the host galaxy. However, NGC3081, NGC3185, NGC3281, NGC5273, and NGC7743 deviated from this correlation.

4 DISCUSSION AND CONCLUSION

We report photometric analysis of Seyfert galaxies using the recently discovered parameter central intensity ratio. The CIR shows good correlations with many structural parameters of host galaxies, especially with the mass of the SMBHs residing at the centre of galaxies (Aswathy & Ravikumar 2018, 2020). For Seyfert galaxies also, the CIR shows strong anti-correlation with the mass of SMBHs. However, the massive SMBHs hosted by ellipticals in the sample display a distinct trend from that displayed by lenticulars and

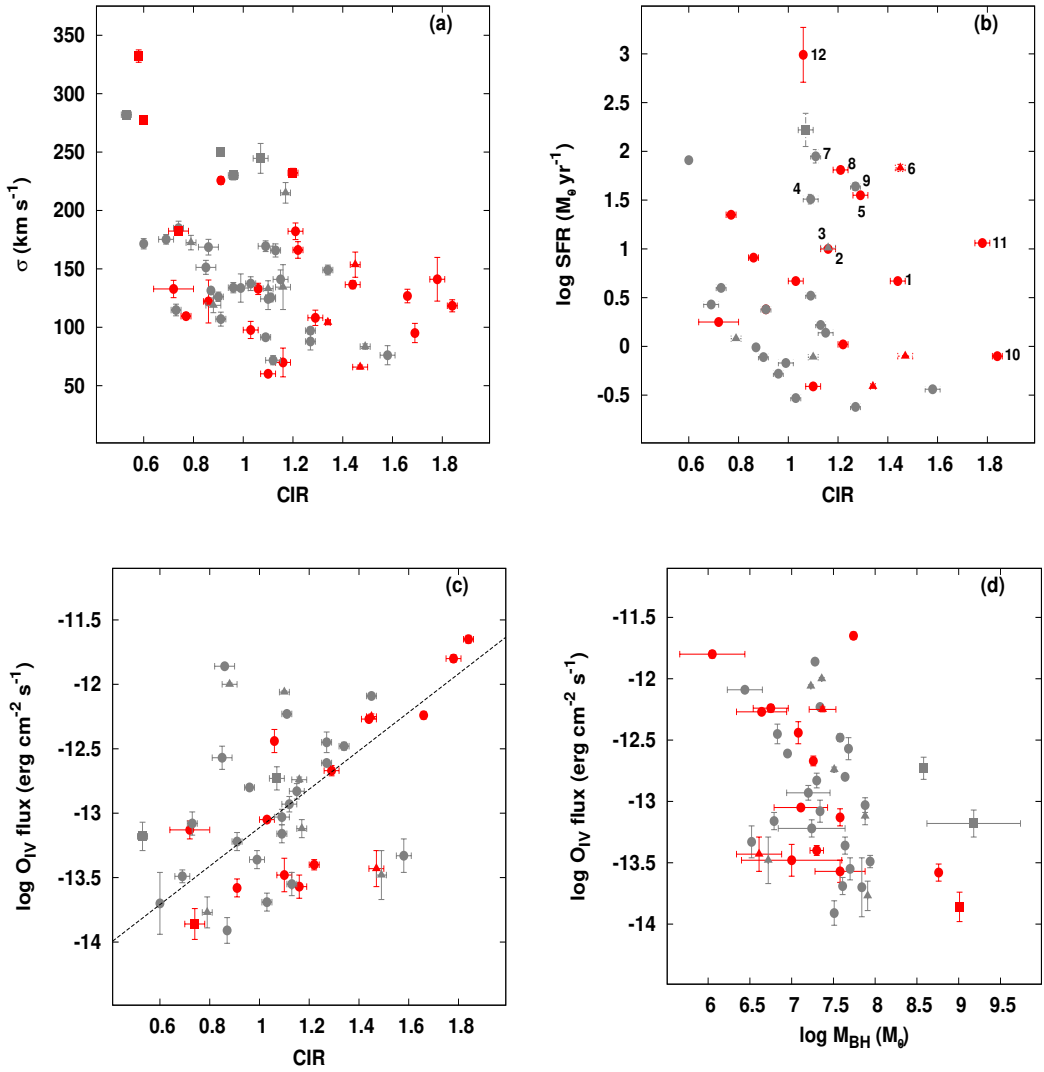


Fig. 2: Variations between the central intensity ratio and (a)stellar velocity dispersion adopted from HyperLEDA database (b)circumnuclear star formation rate (c)OIV flux of AGN and (d)the inter-connection between M_{BH} and OIV flux of the sample galaxies. OIV flux values are taken from (Diamond-Stanic et al. 2009). The symbols used to denote the galaxies are same as Fig. 1.

spirals, in the sense that ellipticals host more massive SMBHs than that hosted by lenticulars and spirals. The disky systems are indistinguishable in the correlation. It is possible that the more massive the central SMBH, the higher the suppression of star formation due to feedback (Harrison 2017). As a decrease in the light in the inner aperture reduces the value of CIR, we can expect the anti-correlation between CIR and mass of SMBH.

The AGN feedback mechanism has a significant role in the evolution process of galaxies, in which the energy released by AGN to the surrounding galactic medium halts the cooling of gas in the central region of galaxies and also removes the gas in the form of massive outflows (Morganti 2017). The AGN feedback process is considered a key factor of galaxy evolution and has been included in several simulations and analytical models for years (e.g., Kauffmann & Haehnelt 2000; Di Matteo et al. 2005; Schaye et al. 2015;

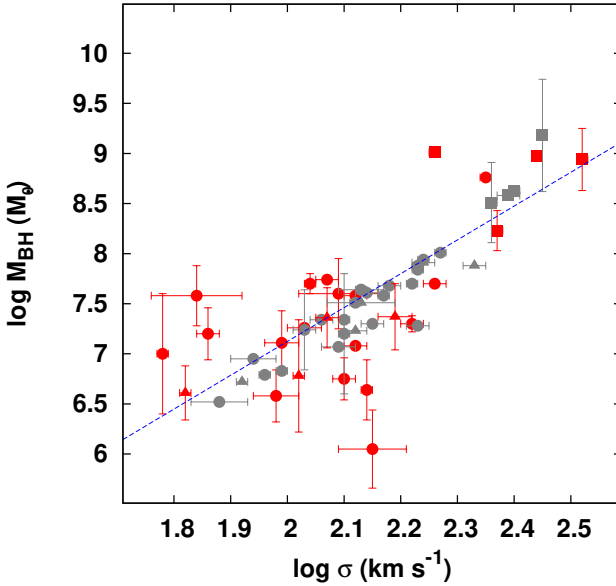


Fig. 3: Variation between stellar velocity dispersion and mass of the SMBH of sample galaxies along with the best fit adopted from Caglar et al. (2020). The symbols used to denote the galaxies are same as in Fig. 1.

Sijacki et al. 2015). This feedback may suppress the star formation at the central part of the galaxy and may decrease or stall completely the growth of the SMBH (e.g., Croton et al. 2006; Sijacki et al. 2007), thus setting up a co-evolution scenario for the galaxy and its SMBH (Aswathy & Ravikumar 2018). Around 30 per cent of Seyfert galaxies are reported to possess outflow incidents (Crenshaw & Kraemer 2007; Crenshaw et al. 2003, 2012). The pc scale AGN-driven outflows in the massive galaxies can expel the gas from the nuclear region, which may reduce the gas accretion towards the centre of the galaxy and leads to quenching of star formation at the central region (Morganti 2017). This interesting phenomenon has been observed in optical, UV, and X-ray emissions and could be traced to such outflows using ionized gas and absorption lines (e.g., Veilleux et al. 2005; Bland-Hawthorn et al. 2007; Tadhunter 2008; King & Pounds 2015).

Different studies argued for the probability of AGN feedback by thermal process in the vicinity of the SMBH (e.g., Di Matteo et al. 2005; Springel et al. 2005; Johansson et al. 2009). Simulations of the AGN feedback mechanism suggest that the Compton heating effect can raise the temperature of the the gas at the nuclear region of about 10-35 pc, to $\sim 10^9$ K (e.g., Gan et al. 2014; Melioli & de Gouveia Dal Pino 2015). This AGN heating may also reduce the star formation in the central region of the galaxy, thus the value of CIR.

Stellar velocity dispersion (σ) of the bulge component is strongly connected with the central SMBH (Ferrarese & Merritt 2000; Gebhardt et al. 2000; Tremaine et al. 2002; Gultekin et al. 2009). Active galaxies are also obeying the $\sigma - M_{\text{BH}}$ relation, but with significant scatter (Caglar et al. 2020). It is also reported that CIR of early-type galaxies are well correlated with the stellar velocity dispersion (Aswathy & Ravikumar 2018). In the present study, however, Seyfert galaxies show a large scatter in the CIR – σ relation, even though there is a strong CIR - M_{BH} relation. The uncertainties present in the measurement of stellar velocity dispersion could be high when excessively illuminated by central AGN (Riffel et al. 2013). Furthermore,

stellar velocity dispersion measurements may be skewed due to the rotational effect of stellar disks (Woo et al. 2015). In order to explain further this, we have plotted the variation of M_{BH} with σ in Figure 3. The velocity dispersion measurements for galaxies with dynamical estimation of mass of SMBH available, shown in red, clearly display a larger scatter than that of galaxies without dynamical estimation of M_{BH} (gray points). For the $\sigma - M_{\text{BH}}$ correlation in the combined sample of spirals and lenticulars, we obtained a linear correlation coefficient of $r = 0.65$ with significance, $s > 99.99$ per cent. At the same time, the correlation coefficient of CIR - M_{BH} (for spirals + lenticulars) relation is, $r = -0.74$ with significance, $s > 99.99$ per cent. The scatter of the correlations $\sigma - M_{\text{BH}}$ and CIR - M_{BH} are 2.63 and 2.04 dex respectively, further establishing that the CIR is, in fact, a better tracer of the M_{BH} than the central velocity dispersion.

The observed correlation between CIR and OIV flux, shown in Figure 2(c), also displays the possibility of larger uncertainties present in measurement of emission lines in galaxies associated with AGN (e.g., Lutz et al. 2003; Armus et al. 2006, 2007; Veilleux et al. 2009; Diamond-Stanic et al. 2009). In this case also, the correlation coefficient increases to 0.76 with a significance, $s = 99.38$ per cent if we just consider galaxies with dynamically estimated SMBH masses, but it drops to 0.62 ($s = 99.74$ per cent) when these data points are excluded. Seyfert galaxies with high OIV flux emission possess enhanced nuclear star formation (Diamond-Stanic & Rieke 2012), and an increase in CIR is expected in galaxies with increased OIV emission. However, the OIV flux of the sample galaxies shows only a weak anti-correlation ($r = -0.58$ with $s = 99.95$ per cent) with the mass of SMBH shown in Figure 2(d), possibly due to the increased uncertainties involved in both the quantities.

Generally, Seyfert galaxies can be observed and located through the UV emission coming out from the sources (Rieke 2002). Apart from age and morphological classification, the common feature of Seyfert galaxies is their intense star formation (Cid Fernandes et al. 2004; Sarzi et al. 2007; Davies et al. 2007; Kauffmann & Heckman 2009). We explore the variation of the estimated circumnuclear SFR by the excess UV with CIR, as shown in Figure 2(b). We notice that the galaxies harbouring central structures such as pc scale nuclear dust spiral, nuclear starburst, and the galaxies possessing high SFR are showing large deviation in the observed CIR – SFR relation. The measure of nuclear SFR has been shown to increase from the central region to the outskirts of galaxies (Diamond-Stanic & Rieke 2012; Esquej et al. 2014). The outflow from the central part of the galaxy due to the AGN feedback mechanism can interact with the interstellar medium (ISM) effectively (Ostriker et al. 2010; Weinberger et al. 2017; Yuan et al. 2018). The feedback-driven outflow of gas enhances the star formation at larger radii from the core of the galaxy (Ishibashi et al. 2013; Ishibashi & Fabian 2014). This outflow of gas can be responsible for enhancing the circumnuclear star formation rate. All these can affect measurements of both star formation rate and CIR, rendering a weak correlation between the two.

We employed CIR, to explore the presence of central features in Seyfert galaxies and their role in galaxy evolution. The analysis shows that CIR measured for Seyfert galaxies predicts the mass of central SMBHs even better than the estimates obtained by spectroscopic parameters like the central velocity dispersion. Being a photometric tool, this promises a cheap and fast technique to explore large galaxy samples, which has great potential in observations of new generation facilities like the James Webb Space Telescope.

Acknowledgements We sincerely thank the anonymous referee for her/his comments which had improved the quality of the paper significantly. VKT would like to acknowledge the financial support from the Council of Scientific & Industrial Research (CSIR), Government of India. We acknowledge the use of the NASA/IPAC Extragalactic Database (NED), <https://ned.ipac.caltech.edu/> operated by the Jet Propulsion Laboratory, California Institute of Technology, and the Hyperleda database, <http://leda.univ-lyon1.fr/>. We acknowledge the use of data publicly available at Mikulski Archive for Space Telescopes (MAST), <http://archive.stsci.edu/> observed by NASA/ESA Hubble Space Telescope and Galaxy Evolution Explorer (GALEX) led by the California Institute of Technology <http://galex.stsci.edu/>

References

- Abraham, R. G., Valdes, F., Yee, H. K. C., & van den Bergh, S. 1994, ApJ, 432, 75 2
- Alatalo, K., Lacy, M., Lanz, L., et al. 2015, ApJ, 798, 31 2
- Alexander, D., & Hickox, R. 2012, New Astronomy Reviews, 56, 93 2
- Alonso-Herrero, A., Pereira-Santaella, M., Rieke, G. H., et al. 2013, ApJ, 765, 78 2
- Armus, L., Bernard-Salas, J., Spoon, H. W. W., et al. 2006, ApJ, 640, 204 10
- Armus, L., Charmandaris, V., Bernard-Salas, J., et al. 2007, ApJ, 656, 148 10
- Aswathy, S., & Ravikumar, C. D. 2018, MNRAS, 477, 2399 1, 2, 4, 7, 9
- Aswathy, S., & Ravikumar, C. D. 2020, Research in Astronomy and Astrophysics, 20, 015 2, 7
- Barth, A. J., Ho, L. C., Filippenko, A. V., Rix, H.-W., & Sargent, W. L. W. 2001, ApJ, 546, 205 4
- Beifiori, A., Courteau, S., Corsini, E. M., & Zhu, Y. 2012, MNRAS, 419, 2497 4
- Bertin, E., & Arnouts, S. 1996, A&AS, 117, 393 4
- Bianchi, S., Chiaberge, M., Piconcelli, E., & Guainazzi, M. 2007, MNRAS, 374, 697 6, 7
- Bland-Hawthorn, J., Veilleux, S., & Cecil, G. 2007, Ap&SS, 311, 87 9
- Boer, B., Schulz, H., & Keel, W. C. 1992, A&A, 260, 67 7
- Busch, G., Eckart, A., Valencia-S., M., et al. 2017, A&A, 598, A55 4
- Caglar, T., Burtscher, L., Brandl, B., et al. 2020, A&A, 634, A114 9
- Christensen, L., Jahnke, K., Wisotzki, L., et al. 2006, A&A, 452, 869 2
- Cid Fernandes, Roberto, J., & Terlevich, R. 1995, MNRAS, 272, 423 1
- Cid Fernandes, R., Gu, Q., Melnick, J., et al. 2004, MNRAS, 355, 273 10
- Cid Fernandes, R., Heckman, T., Schmitt, H., González Delgado, R. M., & Storchi-Bergmann, T. 2001, ApJ, 558, 81 1
- Cid-Fernandes, R., Schmitt, H. R., & Storchi-Bergmann, T. 2001, in Revista Mexicana de Astronomia y Astrofisica Conference Series, Vol. 11, Revista Mexicana de Astronomia y Astrofisica Conference Series, 133 6
- Combes, F., García-Burillo, S., Audibert, A., et al. 2019, A&A, 623, A79 4
- Conselice, C. J. 2003, ApJS, 147, 1 2
- Crenshaw, D. M., Fischer, T. C., Kraemer, S. B., Schmitt, H. R., & Turner, T. J. 2012, in Astronomical Society of the Pacific Conference Series, Vol. 460, AGN Winds in Charleston, ed. G. Chartas, F. Hamann,

- & K. M. Leighly, 261 9
- Crenshaw, D. M., & Kraemer, S. B. 2007, in Astronomical Society of the Pacific Conference Series, Vol. 373, The Central Engine of Active Galactic Nuclei, ed. L. C. Ho & J. W. Wang, 319 9
- Crenshaw, D. M., Kraemer, S. B., & George, I. M. 2003, ARA&A, 41, 117 9
- Croton, D. J., Springel, V., White, S. D. M., et al. 2006, MNRAS, 365, 11 9
- Davies, R. I., Müller Sánchez, F., Genzel, R., et al. 2007, ApJ, 671, 1388 7, 10
- Davis, B. L., Graham, A. W., & Cameron, E. 2018, ApJ, 869, 113 4, 5
- Davis, B. L., Graham, A. W., & Cameron, E. 2019, ApJ, 873, 85 5
- Davis, B. L., Berrier, J. C., Johns, L., et al. 2014, ApJ, 789, 124 4
- de Vaucouleurs, G., de Vaucouleurs, A., Corwin, Herold G., J., et al. 1991, Third Reference Catalogue of Bright Galaxies 6
- Devost, D. 2007, in American Astronomical Society Meeting Abstracts, Vol. 210, American Astronomical Society Meeting Abstracts #210, 112.09 7
- Di Matteo, T., Springel, V., & Hernquist, L. 2005, Nature, 433, 604 8, 9
- Diamond-Stanic, A. M., & Rieke, G. H. 2012, ApJ, 746, 168 2, 4, 10
- Diamond-Stanic, A. M., Rieke, G. H., & Rigby, J. R. 2009, ApJ, 698, 623 2, 3, 7, 8, 10
- Dong, A.-J., & Wu, Q. 2015, MNRAS, 453, 3447 4
- Dong, X. Y., & De Robertis, M. M. 2006, AJ, 131, 1236 4
- Dullo, B. T., Knapen, J. H., Williams, D. R. A., et al. 2018, MNRAS, 475, 4670 4
- Dumas, G., Mundell, C. G., Emsellem, E., & Nagar, N. M. 2007, MNRAS, 379, 1249 4
- Ellison, S. L., Patton, D. R., Mendel, J. T., & Scudder, J. M. 2011, MNRAS, 418, 2043 1
- Esquej, P., Alonso-Herrero, A., González-Martín, O., et al. 2014, ApJ, 780, 86 10
- Evans, I. N., Koratkar, A. P., Storchi-Bergmann, T., et al. 1996, ApJS, 105, 93 7
- Ferrarese, L., & Merritt, D. 2000, ApJ, 539, L9 2, 5, 9
- Gadotti, D. A., & Sánchez-Janssen, R. 2012, MNRAS, 423, 877 6
- Gan, Z., Yuan, F., Ostriker, J. P., Ciotti, L., & Novak, G. S. 2014, ApJ, 789, 150 9
- García-Burillo, S., Combes, F., Usero, A., et al. 2014, A&A, 567, A125 2
- Gebhardt, K., Bender, R., Bower, G., et al. 2000, ApJ, 539, L13 2, 9
- Gil de Paz, A., Madore, B. F., Boissier, S., et al. 2005, ApJ, 627, L29 5
- Gil de Paz, A., Madore, B. F., Boissier, S., et al. 2007, ApJ, 661, 115 5
- González Delgado, R. M., Heckman, T., & Leitherer, C. 2001, ApJ, 546, 845 1, 7
- Goulding, A. D., Alexander, D. M., Lehmer, B. D., & Mullaney, J. R. 2010, MNRAS, 406, 597 4
- Graham, A. W., & Soria, R. 2019, MNRAS, 484, 794 4
- Gültekin, K., Richstone, D. O., Gebhardt, K., et al. 2009, ApJ, 698, 198 2, 9
- Häring, N., & Rix, H.-W. 2004, ApJ, 604, L89 2
- Harrison, C. M. 2017, Nature Astronomy, 1, 0165 8
- Heckman, T. M., & Best, P. N. 2014, ARA&A, 52, 589 2
- Ho, L. C. 2008, ARA&A, 46, 475 1
- Ho, L. C., Filippenko, A. V., & Sargent, W. L. 1995, ApJS, 98, 477 1

- Hopkins, P. F., Hernquist, L., Cox, T. J., et al. 2006, ApJS, 163, 1 2
- Hopkins, P. F., Torrey, P., Faucher-Giguère, C.-A., Quataert, E., & Murray, N. 2016, MNRAS, 458, 816 2
- Ishibashi, W., & Fabian, A. C. 2014, MNRAS, 441, 1474 10
- Ishibashi, W., Fabian, A. C., & Canning, R. E. A. 2013, MNRAS, 431, 2350 10
- Izumi, T., Kawakatu, N., & Kohno, K. 2016, ApJ, 827, 81 4
- Johansson, P. H., Naab, T., & Burkert, A. 2009, ApJ, 690, 802 9
- Kauffmann, G., & Haehnelt, M. 2000, MNRAS, 311, 576 8
- Kauffmann, G., & Heckman, T. M. 2009, MNRAS, 397, 135 10
- Kauffmann, G., Heckman, T. M., Tremonti, C., et al. 2003, MNRAS, 346, 1055 1
- Kawakatu, N., Anabuki, N., Nagao, T., Umemura, M., & Nakagawa, T. 2006, ApJ, 637, 104 1
- King, A., & Pounds, K. 2015, ARA&A, 53, 115 9
- Koliopanos, F., Ciambur, B. C., Graham, A. W., et al. 2017, A&A, 601, A20 4
- Koribalski, B. S., & López-Sánchez, Á. R. 2009, MNRAS, 400, 1749 5
- Kormendy, J., & Ho, L. C. 2013, ARA&A, 51, 511 2, 4
- Kormendy, J., & Richstone, D. 1995, ARA&A, 33, 581 5
- Krause, M., Fendt, C., & Neininger, N. 2007, A&A, 467, 1037 2
- López-Sánchez, Á. R. 2010, A&A, 521, A63 5
- Lutz, D., Sturm, E., Genzel, R., et al. 2003, A&A, 409, 867 10
- Magorrian, J., Tremaine, S., Richstone, D., et al. 1998, AJ, 115, 2285 2, 4
- Maiolino, R., Krabbe, A., Thatte, N., & Genzel, R. 1998, ApJ, 493, 650 1
- Marconi, A., & Hunt, L. K. 2003, ApJ, 589, L21 2
- Martini, P., Regan, M. W., Mulchaey, J. S., & Pogge, R. W. 2003, ApJ, 589, 774 7
- McConnell, N. J., & Ma, C.-P. 2013, ApJ, 764, 184 2, 5
- Melioli, C., & de Gouveia Dal Pino, E. M. 2015, ApJ, 812, 90 9
- Morganti, R. 2017, Frontiers in Astronomy and Space Sciences, 4, 42 8, 9
- Morganti, R., Oosterloo, T., Oonk, J. B. R., Frieswijk, W., & Tadhunter, C. 2015, A&A, 580, A1 2
- Muñoz Marín, V. M., González Delgado, R. M., Schmitt, H. R., et al. 2007, AJ, 134, 648 7
- Nowak, N., Thomas, J., Erwin, P., et al. 2010, MNRAS, 403, 646 4
- Onken, C. A., Peterson, B. M., Dietrich, M., Robinson, A., & Salamanca, I. M. 2003, ApJ, 585, 121 4
- Osterbrock, D. E., & Martel, A. 1993, ApJ, 414, 552 2
- Ostriker, J. P., Choi, E., Ciotti, L., Novak, G. S., & Proga, D. 2010, ApJ, 722, 642 10
- Pellegrini, S. 2010, ApJ, 717, 640 4
- Pérez-Ramírez, D., Knapen, J. H., Peletier, R. F., et al. 2000, MNRAS, 317, 234 7
- Pottasch, S. R., Beintema, D. A., Bernard Salas, J., & Feibelman, W. A. 2001, A&A, 380, 684 7
- Pović, M., Sánchez-Portal, M., Pérez García, A. M., et al. 2009, ApJ, 706, 810 1
- Press, W. H., Teukolsky, S. A., Vetterling, W. T., & Flannery, B. P. 1992, Numerical recipes in FORTRAN. The art of scientific computing 6
- Querejeta, M., Schinnerer, E., García-Burillo, S., et al. 2016, A&A, 593, A118 2
- Ramos Almeida, C., Levenson, N. A., Rodríguez Espinosa, J. M., et al. 2009, ApJ, 702, 1127 7

- Rashed, Y. E., Eckart, A., Valencia-S., M., et al. 2015, MNRAS, 454, 2918 2
- Rieke, G. H. 2002, in Astronomical Society of the Pacific Conference Series, Vol. 258, Issues in Unification of Active Galactic Nuclei, ed. R. Maiolino, A. Marconi, & N. Nagar, 113 7, 10
- Riffel, R. A., Storchi-Bergmann, T., Dors, O. L., & Winge, C. 2009, MNRAS, 393, 783 6
- Riffel, R. A., Storchi-Bergmann, T., Riffel, R., et al. 2013, MNRAS, 429, 2587 6, 9
- Salim, S., Rich, R. M., Charlot, S., et al. 2007, ApJS, 173, 267 5
- Sandage, A., & Tammann, G. A. 1987, A Revised Shapley-Ames Catalog of Bright Galaxies 2
- Sarzi, M., Allard, E. L., Knapen, J. H., & Mazzuca, L. M. 2007, MNRAS, 380, 949 10
- Savorgnan, G. A. D., & Graham, A. W. 2015, VizieR Online Data Catalog, J/MNRAS/446/2330 2
- Savorgnan, G. A. D., & Graham, A. W. 2016, ApJS, 222, 10 4
- Schaye, J., Crain, R. A., Bower, R. G., et al. 2015, MNRAS, 446, 521 8
- Shapley, H., & Ames, A. 1932, Annals of Harvard College Observatory, 88, 41 2
- Sijacki, D., Springel, V., Di Matteo, T., & Hernquist, L. 2007, MNRAS, 380, 877 9
- Sijacki, D., Vogelsberger, M., Genel, S., et al. 2015, MNRAS, 452, 575 9
- Silverman, J. D., Kampczyk, P., Jahnke, K., et al. 2011, ApJ, 743, 2 1
- Smajić, S., Moser, L., Eckart, A., et al. 2014, A&A, 567, A119 4
- Smith, J. D. T., Dale, D. A., Armus, L., et al. 2004, ApJS, 154, 199 7
- Springel, V., Di Matteo, T., & Hernquist, L. 2005, MNRAS, 361, 776 9
- Sruthi, K., & Ravikumar, C. D. 2021, MNRAS, 500, 1343 4
- Tadhunter, C. 2008, Mem. Soc. Astron. Italiana, 79, 1205 9
- Terlevich, R., & Melnick, J. 1985, MNRAS, 213, 841 1
- Thilker, D. A., Bianchi, L., Boissier, S., et al. 2005, ApJ, 619, L79 5
- Tremaine, S., Gebhardt, K., Bender, R., et al. 2002, ApJ, 574, 740 9
- van den Bosch, R. C. E. 2016, ApJ, 831, 134 4
- Veilleux, S., Cecil, G., & Bland-Hawthorn, J. 2005, ARA&A, 43, 769 9
- Veilleux, S., Rupke, D. S. N., Kim, D. C., et al. 2009, ApJS, 182, 628 10
- Villforth, C., Sarajedini, V., & Koekemoer, A. 2012, MNRAS, 426, 360 1
- Wang, J., Fabbiano, G., Karovska, M., Elvis, M., & Risaliti, G. 2012, ApJ, 756, 180 2
- Weedman, D. W. 1977, ARA&A, 15, 69 2
- Weinberger, R., Springel, V., Hernquist, L., et al. 2017, MNRAS, 465, 3291 10
- Woo, J.-H., Yoon, Y., Park, S., Park, D., & Kim, S. C. 2015, ApJ, 801, 38 6, 10
- Wylezalek, D., & Zakamska, N. L. 2016, MNRAS, 461, 3724 2
- Yuan, F., Yoon, D., Li, Y.-P., et al. 2018, ApJ, 857, 121 10